RESEARCH ARTICLE

Editorial Process: Submission:10/21/2025 Acceptance:05/31/2026 Published:06/19/2026

Orange Peel Extract-Mediated Green Synthesis of PEG-Modified ZnO Nanoparticles: Structural Characterization, Biocompatibility, and Anticancer Efficacy

Manasa Kodali[1], Subramani Kaloni[2], Rithanya M[1], Koyeli Girigoswami[3]*

Abstract

Objectives: Engineered nanomaterials could potentially interact with biomolecules and intracellular processes, as many biological activities take place at the nanoscale level. Conventional anticancer therapies have several limitations, which warrant the introduction of alternative cancer cell killing agents. **Methods:** In the present study, we have synthesized ZnO nanoparticles using orange peel extract and encapsulated them inside polyethylene glycol (PEG), a biocompatible polymer (PEG-ZnO-OP). Different characterization techniques were performed to ensure the proper synthesis of the nanoparticles. The biocompatibility was assessed by the MTT assay using normal fibroblast cells, 3T3L1, hemolysis assay, and zebrafish embryo studies. Finally, the anticancer activity in vitro was estimated by the MTT assay in the lung cancer cell line. **Results:** The hydrodynamic diameter and zeta potential were 43 nm and -20 mV, respectively, showing an ultrasmall size and moderate stability in an aqueous environment. The XRD data suggested a good crystalline structure; SEM and EDX showed size distribution between 81 nm and 143 nm, and the presence of Zn and O, along with other trace elements, was probably contributed by the orange peel extract. The PEG-ZnO-OP nanoparticles were highly biocompatible up to a dose of 50 µg/mL, as assessed both in vitro and in vivo. Further, the anticancer activity showed a high cell killing effect with an IC_{50} value of 43.88 µg/ml. **Conclusion:** This study demonstrated that our synthesized PEG-ZnO-OP nanoparticles were safe to administer and could cause significant cancer cell killing. Future studies involving the anticancer effect in other cell lines and animal models need further exploration.

Keywords: zinc oxide nanoparticles- orange peel extract- zebrafish embryos- anticancer activity- healthcare

Asian Pac J Cancer Prev, **27 (6)**, 2163-2174

Introduction

Metal and metal oxide nanoparticles have been explored for their various biomedical applications [1-4], and among them, zinc oxide is studied the most [5]. Zinc oxide is a semiconducting inorganic material with three different crystal structures: wurtzite, zinc blende, and rock salt. At ambient conditions, the structure of wurtzite is thermodynamically stable, with every zinc atom being tetrahedrally coordinated with four oxygen atoms [6]. With a wide band gap of 3.1–3.3 eV [7, 8], zinc oxide has great potential for application in many fields, such as biosensors, cosmetics, drug carriers, photocatalysts, anti-amyloid agents, and antibacterial agents [9-13]. ZnO can be synthesized by many different methods, such as sol–gel processing, homogeneous precipitation, mechanical milling, organometallic synthesis, the microwave method, spray pyrolysis, thermal evaporation, and mechanochemical synthesis [14]. However, these kinds of methods usually use organic solvents and toxic reducing agents, the majority of which are highly reactive and harmful to the environment [15, 16]. Therefore, in order to minimize the impact on the environment, green synthesis processes have been used to synthesize ZnO nanoparticles (ZnO NPs). Green synthesis is a method to produce nanoparticles using microorganisms and plants with biomedical applications. This method has many advantages, such as environmental friendliness, cost-effectiveness, biocompatibility, and safety [17, 18]. Additionally, many studies have proved that ZnO NPs made using green synthesis processes have strong antibacterial and anticancer properties [19].

The orange fruit is one of the most productive fruits in the world. Orange fruit peel, as the main by-product of citrus, is rich in a variety of natural antioxidants and is a known agro-waste. Therefore, the extract of orange

*[1]Saveetha Medical College and Hospital, Saveetha Institute of Medical and Technical Sciences, Thandalam, Chennai, 602105, India. [2]Department of Obstetrics and Gynaecology, Saveetha Medical College and Hospital, Saveetha Institute of Medical and Technical Sciences, Thandalam, Chennai, 602105, India. [3]Medical Bionanotechnology Lab, Department of Obstetrics and Gynaecology, Saveetha Medical College and Hospital, Saveetha Institute of Medical and Technical Sciences, Thandalam, Chennai, 602105, India. *For Correspondence: koyelig@gmail.com*

peel is considered to be used as a stabilizer to prepare ZnO NPs [20]. However, ZnO NPs green synthesis based on extracts of orange fruit peel has not studied fully. Particularly, the influence of pH value and annealing temperature on the morphology and properties of ZnO NPs by green synthesis till lacks of understanding. Moreover, to obtain a sustained release of these nanoparticles over a duration of time, we need to encapsulate them in a benign biopolymer [21, 22]. Polyethylene glycol (PEG) is extensively utilized as a covalent modulator of particles and biological macromolecules and as a carrier for low molecular weight medications [23]. PEG exhibits minimal antigenicity and immunogenicity, exceptional solubility in water-based solutions, and minimal toxicity [24-26]. This polymer is recognized as non-biodegradable; however, it can be rapidly excreted following administration to living organisms. The presence of PEG in water-based solutions is not associated with any harmful impact on the structure or functioning of enzymes or proteins. PEG also demonstrates exceptional biodistribution and pharmacokinetic characteristics [27]. Following infusion into animals, the substance exhibits prolonged existence in the bloodstream and minimal aggregation in the spleen, liver, and other reticuloendothelial system organs [28, 23]. The antibacterial, anticancer, and UV-blocking qualities of zinc oxide (ZnO) nanoparticles make them one of the most promising nanomaterials [5, 29]. However, depending on stabilizers, surface modifications, and synthesis techniques, their interactions with biological systems can differ. It is common practice to modify their surfaces with biocompatible substances like PEG to increase their compatibility with living cells and tissues. PEG-entrapped ZnO nanoparticles are therefore being explored more and more for biomedical uses; nonetheless, a thorough assessment of their biosafety is necessary [30].

There are many types of conventional cancer therapies, like surgery, chemotherapy, and radiotherapy, that remain foundational in oncology but possess notable drawbacks. Surgery is effective for localized tumors but often fails against metastasis and can lead to complications and incomplete clearance of the tumour, leading to recurrence. The other aspects of conventional therapy are chemotherapy and radiotherapy, which target rapidly dividing cells. However, these therapeutic modalities lack specificity, and damage the healthy tissues also. Post intervention, they cause systemic toxicities such as hematologic, gastrointestinal, and organ damage. In another aspect, drug resistance and heterogeneous composition of the tumors frequently reduce the long-term effectiveness of these treatments. Radiation precision improvements still struggle with resistant tumor regions and normal tissue injury. These limitations underscore the need for more targeted and personalized therapies, and also the incorporation of supportive cell-killing strategies involving nanoparticles [31]. Cancer nano vaccines have also shown their effectiveness in controlling the cancerous cell division [32]. Green nanotechnology uniquely contributes to cancer therapy by enabling eco-friendly synthesis of biocompatible nanoparticles, reducing toxicity, improving targeted drug delivery, enhancing therapeutic efficacy, and promoting sustainable, inert anticancer strategies [33].

The aim of the present study is to prepare the orange peel aqueous extract, filter, and characterize for its constituents using phytochemical analysis and GC-MS analysis. Further, using this extract, ZnO NPs were synthesized using the precipitation method and entrapped in PEG, followed by characterization using various photophysical tools (PEG-ZnO-OP). The hydrodynamic diameter and stability are estimated by dynamic light scattering (DLS) and zeta potential analysis, respectively. The absorption peak and characteristic bond formations were analyzed using UV-visible absorption spectroscopy and FTIR analysis, respectively. The crystalline structure was confirmed by XRD analysis. The surface morphology and structure of the as-synthesized ZnO NPs were characterized using scanning electron microscopy (SEM), and EDX was used to identify the composition of the green-synthesized ZnO NPs. A step forward, the in vitro biocompatibility of the synthesized nanoparticles was assessed using normal fibroblast cell lines, 3T3L1, and a haemolysis assay. In vivo biocompatibility was assessed using zebrafish embryos, and further, the anticancer activity was monitored using the lung cancer cell line, A549.

Materials and Methods

Materials

Zinc nitrate hexahydrate, sodium hydroxide, potassium bromide, DMEM, antibiotics-antimycotic solution, trypsin, PBS tablets (pH= 7.4), and other reagents were purchased from HiMedia Pvt. Ltd, India. Foetal bovine serum (FBS) was procured from Gibco, USA, and the cells (3T3-L1 and A549) were ordered from NCCS, Pune, India.

Extraction of orange peel

Orange peel extract was used as a stabilizing and reducing agent in the green synthesis of PEG-entrapped ZnO nanoparticles. Freshly peeled orange peels were shade dried for 10-12 days until all the moisture was removed (appeared crispy), followed by powder making using a grinder. To make the extract, orange peel powder was measured to a concentration of 0.25% in distilled water. The mixture was ultrasonicated four times at 50 Hz for 15 minutes. After that, it was agitated for an hour at 70–75°C at 500 rpm using a magnetic stirrer. To get a homogenous solution without any big granules, the extract was then filtered through Whatman filter paper. The solution was pale yellow in colour, and the extract yield ranged from 30-35%. The filtered extract was sealed in a 50 ml tube, sealed with parafilm, and stored at 4 ^{o}C until further use.

Phytochemical analysis and GC-MS Analysis of the orange peel extract

To determine the presence of bioactive chemicals, a phytochemical analysis of the orange peel extract was carried out using the methodology outlined by Garg and Garg (2018) [34]. A number of qualitative tests were performed on the freshly made extract in order to identify different phytochemicals. Saponins were identified using

the foam test, and the presence of tannins was verified using the ferric chloride test and Braymer's test. Mayer's test and the sulfuric acid test were used to identify alkaloids, while the Salkowski test was used to detect terpenoids. The alkaline reagent test and the sodium picrate test were used to confirm flavonoids. The NaOH and Molisch tests were used to identify carbohydrates. These phytochemical constituents play a vital role in the reduction and stabilization of nanoparticles during the green synthesis process.

GC-MS analysis of the aqueous orange peel extract was performed to identify the metabolites present in the sample. The analysis was conducted using an Agilent Technologies 7890B gas chromatograph coupled with a 5977B mass spectrometer according to Guttapalli et al. [35]. The aqueous extract was dried using a rotary evaporator and reconstituted in ethanol for GC-MS analysis. The identification of compounds was based on their retention times, fragmentation patterns, and comparison with reference spectra using the NIST-based automated mass spectral deconvolution and identification software.

Synthesis of ZnO nanoparticles using orange peel extract

The ZnO nanoparticles were synthesized using a precipitation method [8]. In this process, 5 mL of 10 millimole zinc nitrate solution was mixed with 50 mL of orange peel extract and stirred using a magnetic stirrer at 500 rpm for 30 minutes at room temperature (25 ºC). Subsequently, 0.5 g of NaOH was gently added to the mixture, and stirring was continued for 2 hours to facilitate the reaction. The beaker was then covered and kept undisturbed overnight at room temperature. The next day, a precipitate was observed, indicating the formation of ZnO nanoparticles. The precipitate was centrifuged three times using distilled water at 5000 rpm for 15 min each to remove impurities, and the pH was measured as 7.2 when dispersed in water, ensuring the removal of excess alkali. The resulting residue was dried in a porcelain crucible at 200 °C, followed by calcination at 250°C for 3 h. The final dried product was ground using a mortar and pestle to obtain a fine powder, which was the desired ZnO nanoparticle sample.

PEG encapsulation

PEGylation of ZnO nanoparticles was done according to Girigoswami et al. [8]. For PEG encapsulation, 5 grams of PEG was dissolved in 100 milliliters of distilled water and was stirred for 30 min at 500 rpm using a magnetic stirrer to make a homogenous PEG solution. Ten milligrams of ZnO nanoparticle powder, which is obtained in the previous step, is combined with ten milliliters of a 5% PEG solution. In order to produce consistent PEG encapsulation around the ZnO nanoparticles, this mixture was then ultrasonically sonicated four times for 15 minutes each time. This step yielded our final product, which was PEG encapsulated ZnO nanoparticles. Until it was needed again, the finished PEG-entrapped ZnO nanoparticle product was kept at 4°C. The steps of synthesis are depicted in Scheme 1.

Characterization of the as-synthesized PEG encapsulated ZnO nanoparticles

The characterizations were done according to Girigoswami et al. 2024. [9]. The PEG-entrapped ZnO nanoparticle sample was characterized by preparing a diluted solution and analyzing it using Dynamic Light Scattering (DLS), zeta potential, and UV-visible absorption, using Malvern Panalytical Ltd. ZS XPLORER, and JASCO V-730 spectrophotometer, respectively. This allowed for the determination of the hydrodynamic diameter, surface charge stability, and absorption spectrum, respectively. Five milliliters of this product were taken, dried completely using a dry heat hot plate maintained at 90 ºC and ground using a mortar pestle to use for characterization in order to do scanning electron microscopy (SEM) and EDX, X-ray diffractometry (XRD), and Fourier Transform Infra-Red spectroscopy (FTIR) analysis. To evaluate the crystalline structure, X-ray diffraction (XRD) examination was performed on a dry powder sample of the nanoparticles using a Unique D8 diffractometer. To guarantee a clean surface for imaging in Scanning Electron Microscopy (SEM), a thin layer of the nanoparticle sample was applied to carbon tape and allowed to dry in a dust-free environment. The SEM analysis was done after subjecting the sample to a Palladium and Gold alloy coating and analysis using Thermo Fisher, FEI QUANTA 250 FEG. The EDX analysis was done to confirm the presence of the elements in the prepared sample. To determine the functional groups and interactions in the sample, FTIR analysis was performed utilizing potassium bromide (KBr) pellet

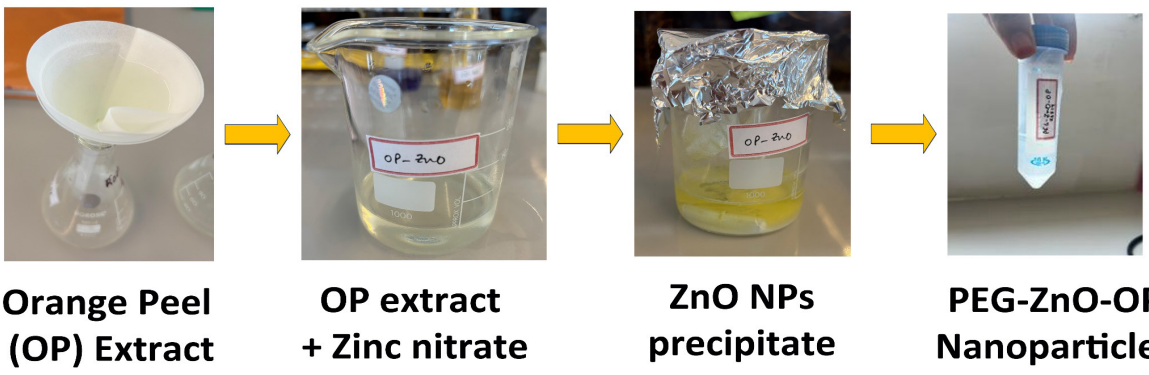

Scheme 1. The Steps of Synthesis of PEGylated ZnO Nanoparticles Using Orange Peel Aqueous Extract (PEG-ZnO-OP)

production using Bruker Alpha FTIR. The spectrum data were recorded in transmission mode.

In vitro and in vivo biocompatibility

MTT assay was performed 24 h after exposure to different doses of PEG-ZnO-OP using 3T3-L1 cells according to Guttapalli et al. [35]. Hemolysis assay was performed using human blood after getting approval from the Institutional Ethics Committee (005/07/2025/IEC/SMCH), Saveetha Medical College and Hospitals, Thandalam, Chennai, India, and getting informed consent from a healthy male volunteer of age 21 years. The experiment was performed according to our previous work [35], and the Declaration of Helsinki was followed.

In vivo biocompatibility was performed using zebrafish embryos after getting permission from the Institutional Animal Ethics Committee (IAEC approval No. SU/CLAR/RD/19/2025), Saveetha Medical College and Hospital, SIMATS. The protocol followed was strictly as done earlier [9].

Anticancer activity using A549 cells

Monitoring of the cancer cell killing capacity of PEG-ZnO-OP was done using the MTT assay. The lung cancer cell line, A549, was utilized for the study. The stock solution of the PEG-ZnO-OP nanoparticles was prepared (1 mg/mL) and filtered using a syringe filter inside a level II biosafety cabinet. 24 h post subculturing of the exponentially growing A549 cells seeded in a 96-well plate, the cells were treated with different doses of these nanoparticles. Incubation was done for a further 24 h, and the MTT assay was performed according to Girigoswami et al. [9]. The percentage of cell killing was calculated against untreated A549 cells, which were taken as the control.

Statistical analysis

Paired Student's t-test was employed to calculate the level of significance compared to the untreated control. The number of replicates was three for all the analyses. The free version of the software Jamovi was used to calculate the level of significance. $p < 0.05 \rightarrow$ statistically significant, was taken as the threshold.

Results

Components of orange peel extract

The phytochemical analysis revealed that the aqueous extract of orange peel contains tannins, flavonoids, glycosides, alkaloids, coumarins, and proteins (Figure 1a).

GC-MS analysis reveals the presence of five lead compounds (Figure 1 b), which are Silane,

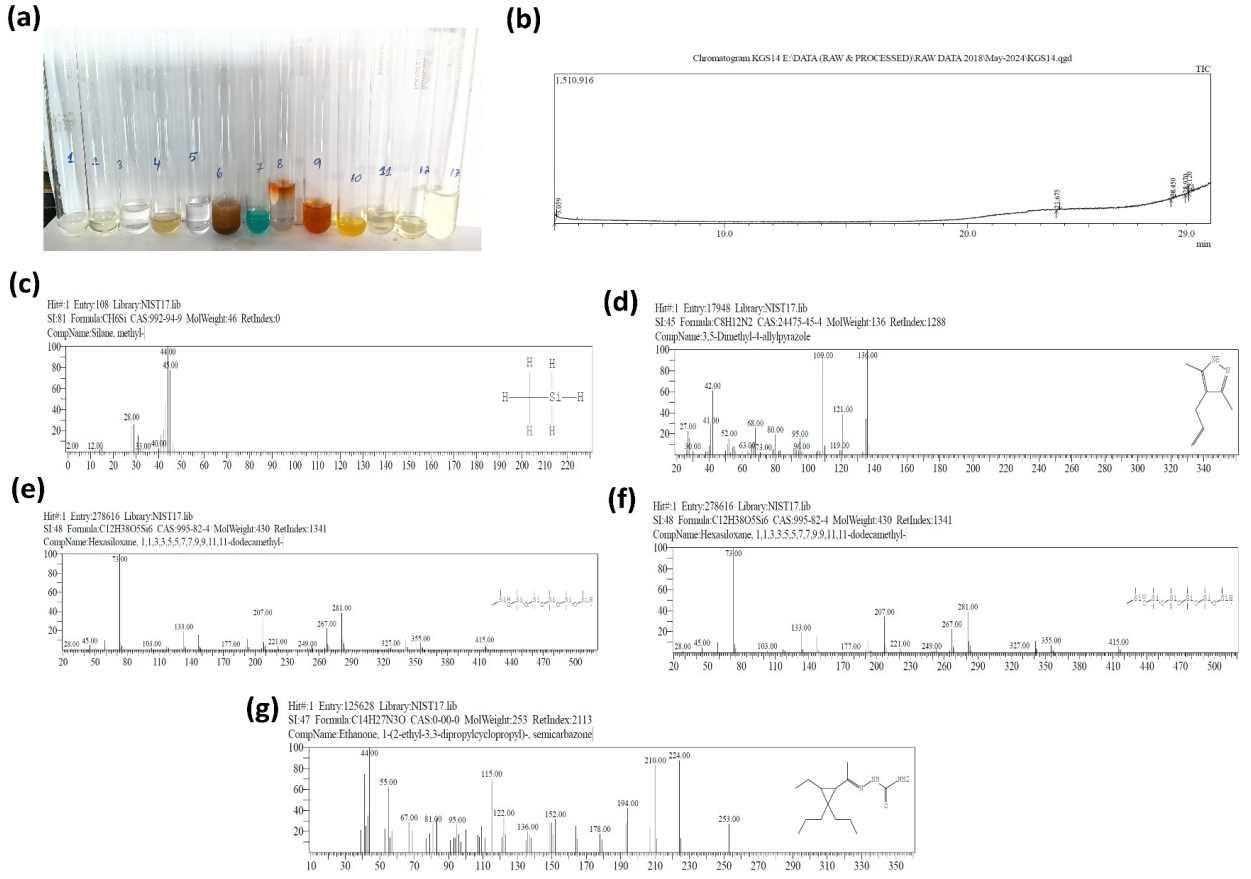

Figure 1. (a) The Phytochemical Analysis for Orange Peel Aqueous Extract. Tubes from left to right indicate tannins, terpenoids & steroids, saponins, flavonoids (ferric chloride test), flavonoids (alkaline test), carbohydrates, reducing sugar, glycosides, alkaloids, polysaccharides, coumarins, quinones, protein, respectively. (b) GC-MS spectrum of orange peel aqueous extract. (c)-(g) Indicates the individual GC-MS spectra for the components of orange peel extract: Silane, methyl-, 3,5-Dimethyl-4-allylpyrazole, Hexasiloxane, 1,1,3,3,5,5,7,7,9,9,11,11-dodecamethyl-, 2-Propanol, 1-[(2-hydroxyethyl)thio]-3-phenoxy-, Ethanone, 1-(2-ethyl-3,3-dipropylcyclopropyl)-, semicarbazone, respectively.

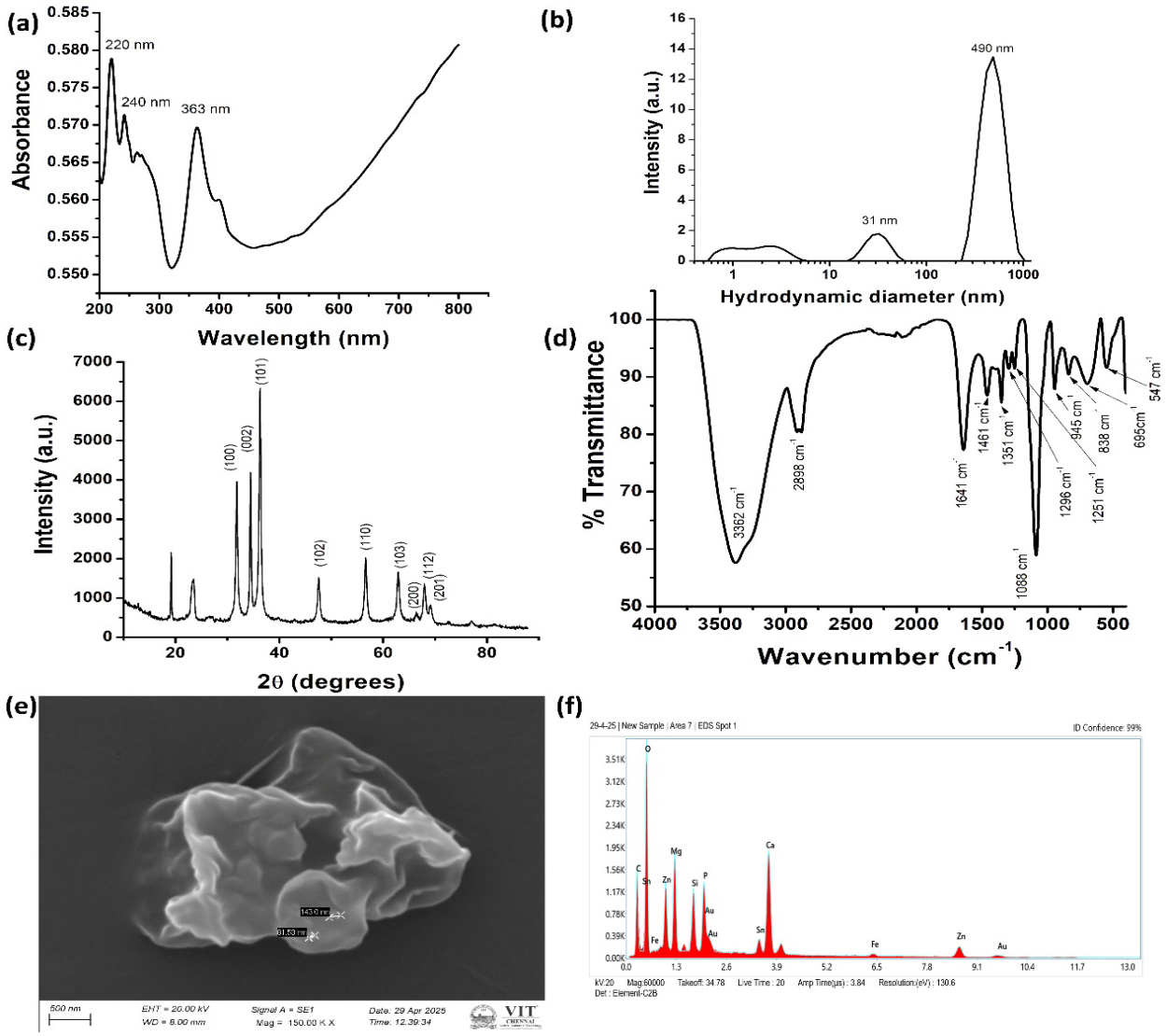

Figure 2. (a) The UV-visible spectrum, (b) hydrodynamic diameter, (c) XRD spectrum, (d) FTIR spectrum, (e) SEM image, and (f) EDX analysis of as-synthesized PEG-ZnO-OP nanoparticles.

methyl-, 3,5-Dimethyl-4-allylpyrazole, Hexasiloxane, 1,1,3,3,5,5,7,7,9,9,11,11-dodecamethyl-, 2-Propanol, 1-[(2-hydroxyethyl)thio]-3-phenoxy-, Ethanone, and 1-(2-ethyl-3,3-dipropylcyclopropyl)-, semicarbazone represented in Figure 1c-g, respectively. The respective abundance, chemical formula, and molecular weight are provided in detail in Table 1.

Characterization of the synthesized PEG-ZnO-CO nanoparticles

The UV-visible spectra showed multiple peaks in the UV region (220 nm, 240 nm, 363 nm) (Figure 2a). The hydrodynamic diameter was found in two regions: 31 nm and 491 nm (Figure 2 b). However, the XRD analysis (Figure 2 c) showed that the crystal size was 43 nm and the peaks present in the diffractogram matched with the JCPDS card number 80-0075, representing ZnO nanoparticles in their hexagonal phase [36].

The zeta potential of the nanoparticles was found to be -20.21 mV, indicating a good stability [37-39]. The FTIR peaks for PEG-ZnO-OP nanoparticles are shown in Figure 2d at wavenumbers 3362 cm^{-1}, 2898 cm^{-1}, 1641 cm^{-1}, 1461 cm^{-1},1351 cm^{-1},1296 cm^{-1}, 1251 cm^{-1}, 1088 cm^{-1}, 945 cm^{-1}, 838 cm^{-1}, 695 cm^{-1}, and 547 cm^{-1}. Table 2 shows

Table 1. The Components of the Aqueous Extract of Orange Peel were Revealed by GC-MS Analysis.

Peak #	Compound Name	Chemical Formula	Molecular Weight	% Abundance
1	Silane, methyl-	CH6Si	46	37.34
2	3,5-Dimethyl-4-allylpyrazole	C8H12N2	136	12.22
3	Hexasiloxane, 1,1,3,3,5,5,7,7,9,9,11,11-dodecamethyl-	C12H38O5Si6	430	11.32
4	2-Propanol, 1-[(2-hydroxyethyl)thio]-3-phenoxy-	C11H16O3S	228	13.33
5	Ethanone, 1-(2-ethyl-3,3-dipropylcyclopropyl)-, semicarbazone	C14H27N3O	253	25.79

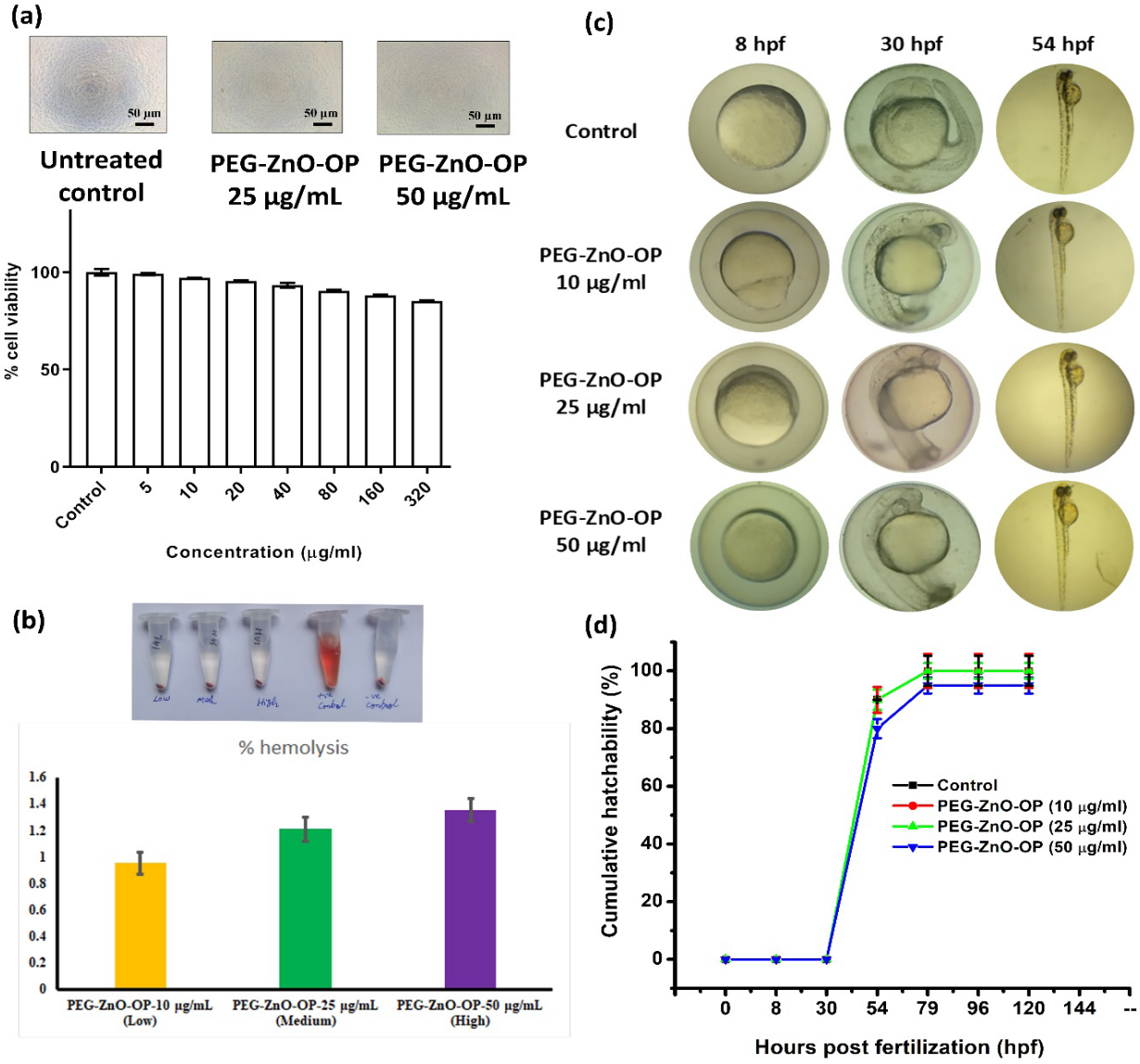

Figure 3. (a) The inverted microscopic images and cell viability using MTT assay for 3T3-L1 cells, 24 h after exposure to different doses of as-synthesized PEG-ZnO-OP nanoparticles. (b) The percentage of haemolysis caused by 2 h incubation with 10 µg/mL (low), 25 µg/mL (medium), and 50 µg/mL (high) doses of as-synthesized PEG-ZnO-OP nanoparticles. (c) The bright field microscopic images (4 X) of zebrafish embryos exposed to 10 µg/mL (low), 25 µg/mL (medium), and 50 µg/mL (high) doses of as-synthesized PEG-ZnO-OP nanoparticles, at different hours post fertilization (hpf). (d) The cumulative hatchability of the embryos after treatment with different doses of the nanoparticles.

the description of bonds corresponding to these peaks.

The SEM image of the PEG-ZnO-OP nanoparticles (Figure 2e) showed the particle size in the range of 81-143 nm and the elemental analysis is shown in Figure 2f.

Biocompatibility of PEG-ZnO-OP nanoparticles

The cell viability of normal fibroblasts, 3T3-L1, as assessed using MTT assay is shown in Figure 3a. Figure 3b shows the haemolysis assay results after treatment with PEG-ZnO-OP nanoparticles at different doses.

Table 2. The FTIR Peaks for PEG-ZnO-OP Nanoparticles and Their Corresponding Bonds

S. No.	Peaks	Bond
1	3362 cm^{-1}, and 2898 cm^{-1}	Stretching of the hydroxyl bond
2	1641 cm^{-1}, 1461 cm^{-1}	amide I–II peaks corroborating the carbonyl stretching of proteins present in orange peel. [40]
3	1296 cm^{-1}, and 1251 cm^{-1}	C-OH stretching vibrations [41]
4	1088 cm^{-1}, 1351 cm^{-1}	C-O bending vibrations at 1351 cm^{-1} [42]. C-O-C peak for PEG at 1088 cm^{-1} [43].
5	945 cm^{-1}	vibration of the C-N bond of the primary amine [44]
6	547 cm^{-1}, 695 cm^{-1}, and 838 cm^{-1}	metal-oxygen (ZnO stretching and vibrations) [44] [41]

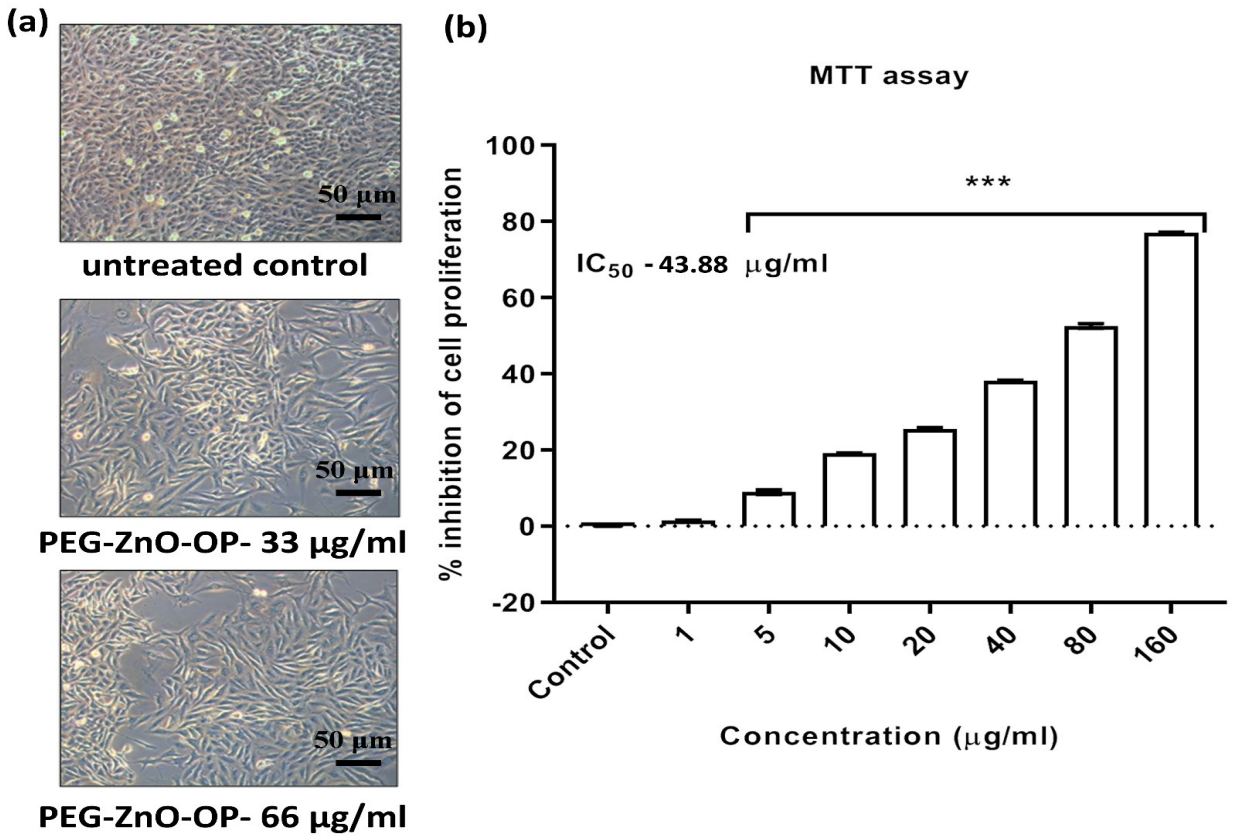

Figure 4. (a) The inverted microscopic images of A549 cells and (b) the cell proliferation inhibition as assessed by MTT assay for A549 cells 24 h post exposure to different doses of PEG-ZnO-CO nanoparticles. (***p<0.001, compared to untreated control)

Figure 3c shows the zebrafish embryo images captured using light microscope after treatment with various doses of PEG-ZnO-OP nanoparticles. Figure 3d shows the cumulative hatchability of the embryos post treatment with PEG-ZnO-OP nanoparticles.

Anticancer activity assessment

The inverted microscopic image of the cells in control (untreated) and after treatment with different doses of PEG-ZnO-OP nanoparticles is shown in Figure 4a. Figure 4b shows the percentage of cell inhibition of A549 cells after PEG-ZnO-OP nanoparticles treatment at different doses.

Discussion

The phytochemical and GC-MS analysis is shown in details in Figure 1 (a-g). Polyphenols present in the extract are responsible for the reduction of zinc nitrate to ZnO. The biochemical reduction reaction takes place via intermediates known as layered basic zinc salts (LBZs), which only later transform to the oxide phase. Solid-phase transformation occurs as Zn(NO3)2·6H2O → LBZN (N: nitrate) → ZnO with no evidence of dissolution [45]. In a previous study, the polyphenols present in pepper extract were used to synthesize ZnO nanoparticles [46]. In Chinese medicines, nanoparticles are been used as a part of traditional medicine [47].

The GC-MS showed the chemical components present in the orange peel (Table 1). Abdelazem et al. in a previous study have shown the presence of alkaloids, total phenolics, total flavonoids, tannins, and saponins in both ethanolic and aqueous extracts of orange peel [48]. Similarly, in another study, the total phenolic content and total flavonoid content were estimated for 80 % ethanolic, acetone, and methanolic extracts of peels of different citrus fruits, including orange. The results revealed that maximum TPC and TF were obtained for the 80 % ethanolic extract compared to acetone and methanol [49]. Akinlabu et al. attempted to extract oil from the agro-waste, orange peel, and found that the oil was rich in alkaloids, tannin, phenol, flavonoid, quinones, carbohydrate, steroids, glycosides, and saponin. These results have shown a similar finding to our extract composition [50]. Oligie et al. made a methanolic extract of sweet orange peel, and the GC-MS analysis found major peaks for 17-octadecynoic acid, 8-methyl-6-nonenoic acid, and pentadecanoic acid [51].

The multiple absorption peaks obtained in UV-visible spectrum (Figure 2a) demonstrated the UV light scavenging property of ZnO nanoparticles due to their semiconducting nature. Only ZnO nanoparticles exhibit semiconducting nature, whereas bulk ZnO does not hold this property [52, 53].

The DLS size (Figure 2b) of 31 nm and 491 nm may be indicative of two separate estimations, the smaller

one representing only ZnO nanoparticles, which were not trapped inside the polymer, and the size of the polymer-entrapped ZnO nanoparticles was 491 nm. The XRD data (Figure 2c) revealed the crystal size to be 43 nm (Scherrer's formula), and the peaks indicated ZnO hexagonal phase [36]. There was a presence of distinct diffraction peaks in the plane (1 0 0), (0 0 2), (1 0 1), (1 0 2), (1 1 0), (1 0 3), (2 0 0), (1 1 2) and (2 0 1), respectively, representing that of ZnO nanoparticles [8]. A similar peak for XRD was found by previous researchers [54, 55].

The zeta potential value was -20.21 mV showing good stability in aqueous environment. For reducing the toxicity of ZnO nanoparticles, PEG coating is applied, and the coating increases the stability of the nanoparticles, evidenced by an increase in their zeta potential [56]. Hence, PEG coating not only stabilizes the structure but also blocks non-specific interactions. The PEG-coated ZnO nanoparticles also exhibited reduced toxicity in rat liver BRL-3A cells, compared to only ZnO, indicating the controlled toxic effect due to polymer coating [56]. The FTIR peaks (Figure 2d) obtained are shown in Table 2 and the respective peaks are also explained. In a previous study, it was clearly reported that PEG contributes a C-O-C peak at 1089 cm^{-1}, and we have also obtained a peak at 1088 cm^{-1}, indicating the presence of PEG. Calibration plots correlating the intensity of the C–O–C absorption band with PEG unit concentration were constructed for PEG samples with different molecular weights (0.4, 5, and 20 kDa). In every case, the absorbance of the C–O–C band at 1089 cm^{-1} showed a linear relationship with PEG concentration up to 1 M. In addition, changes in pH within the range of 4–10 and variations in PEG molecular weight had only a negligible influence on the slope of the calibration curves. These results confirm that the FTIR method, using the C–O–C band at 1089 cm^{-1}, is a reliable and analytically useful approach for determining PEG content [43]. Pure Zn-O stretching is assigned at 544 cm^{-1} [57], whereas we have obtained the peak at 547 cm^{-1}. The shift can be attributed to the incorporation of ZnO inside the PEG, which caused a shift towards a higher wavenumber.

The SEM images showed a proper nano-sized synthesis (Figure 2e) having particle size range from 81 to 143 nm. The polymeric PEG matrix exhibits a distinct layered morphology, over which spherical ZnO nanoparticles are uniformly distributed. These nanoparticles are predominantly located on the surface of the PEG layers and display moderate aggregation, suggesting partial particle–particle interaction while remaining well stabilized within the polymer framework. The elemental analysis (Figure 2f) showed the presence of Zn and O, indicating the presence of ZnO. Moreover, the other elements present indicated the PEG components, and the presence was due to the carbon tape used for preparing the samples. Au and Pd indicated the conductive coating done during the SEM analysis. Other trace elements like Mg, P, Si, Sn, and Fe may be contributed from the orange peel extract.

Any nanostructure, if used for human or environmental purpose should be checked for its biocompatibility in order to render safety to the individuals. We have attempted to monitor the safe dose of the synthesized PEG-ZnO-OP nanoparticles, which can be used safely without harming the normal cells or aquatic animals. The in vitro MTT data using fibroblast cell lines (Figure 3 a) inferred that the cell viability was more than 94 % after treatment with 320 μg/mL of the nanoparticles, revealing their benign nature up to that dose. On the other hand, the hemolysis assay (Figure 3 b) showed that there was less than 2 % haemolysis after exposure to 50 μg/mL of the nanoparticles, indicating that the hemolysis percentage was within the safety limits up to this dose. It is documented that up to 5 % haemolysis is allowed for any lead molecule or drug to be applied safely for humans [58, 59]. Thus, our product was safe to be used up to a dose of 50 μg/mL. In vivo toxicity assay evaluated using zebrafish embryos (Figure 3 c) suggested that up to a dose of 50 μg/mL of the nanoparticles, there was no visible developmental toxicity observed. There was no delay in hatching or development of pericardial edema, tail bent, or any other abnormality. The cumulative hatchability (Figure 3 d) also suggested that up to 95 % of the embryos were alive and hatched at the proper time, similar to the untreated control after treatment with 50 μg/mL of PEG-ZnO-OP nanoparticles. These results altogether suggested that the dose 50 μg/mL was safe to be used for both in vitro as well as in vivo. In a previous study, it was found that the ZnO nanoparticles did not alter the survival of the zebrafish embryos up to a dose of 100 μg/mL, and the hatching was 100 % up to 50 μg/mL of ZnO NP exposure, whereas the delayed hatching was observed at 100 μg/mL [60]. This indicated that our results corroborated with a previously published study. The haemolysis assay is superior compared to the MTT assay because in the MTT assay, the toxicity is assessed using cell lines, which are cultured outside the body. They grow in a controlled environment, and do not get the exact physiological cues like the human body. On the other hand, the haemolysis assay involves blood taken from the human body, which contains all the components present in the human body and is much more physiologically relevant [59]. Hence, we performed both assays to ensure the bio-inertness of our product.

Lung cancer is a leading cause of cancer, with its treatment strategy yet to be established. The treatment varies from case to case, and several treatment strategies have been proposed [61]. In this study, the lung cancer cell line, A549, was used to study the cancer cell-killing effect of the as-synthesized PEG-ZnO-CO nanoparticles. Figure 4 shows that the cell killing was achieved for A549 cells 24h after exposure to different doses of our nanoparticles. The inverted microscopic images (Figure 4a) depicted that the cell density is reduced after exposure to 33 μg/mL and 66 μg/mL, compared to the untreated control. Figure 4 b showed that the percentage of cell growth inhibition increased with an increase in the dose of exposure to PEG-ZnO-OP nanoparticles. The IC_{50} was found to be 43.88 μg/mL. This dose is safe for administration as evidenced by the in vitro and in vivo biocompatibility assays. Previous reports exist showing rod-shaped chemically synthesized ZnO nano rods could induce killing of A549 cells with an IC 50 value of 130.95 μg/mL [62]. On the other hand, Rani et al. reported that green-synthesized ZnO NPs using

neem tree leaves elicited A549 cell killing with an IC 50 value of 138.5 µg/mL [63]. These two studies showed a much higher IC_{50} value compared to our results. This can be attributed to the PEG coating of our green synthesized ZnO nanoparticles, where the polymer entrapment could release the zinc ions slowly and in a sustained manner, so that the cell killing effect can contribute for a longer period of time without any aggregation of the nanoparticles. The lower IC_{50} might also be due to better cellular uptake of the PEGylated particles compared to bare ZnO. Thus, with a much smaller dose, we could achieve 50 % cell killing, which is beneficial for human use.

Nanostructures have been explored for their drug delivery applications using different carriers like liposomes [64, 65], micelles [66] and polymers [67]. Green synthesis has reduced the toxic effect of nanoparticles, as reported by many studies [68]. Polymer entrapment has also shown that natural polymers are more biocompatible than the synthetic ones [8]. Recently, ZnO NPs have been successfully synthesized using extracts from plants. Gao et al. [69]synthesized ZnO NPs using Citrus sinensis peel extract and compared them with commercial ZnONPs, and then applied them as nanocoatings on fresh strawberries to evaluate the preservation effect. The high antibacterial and antifungal activities of ZnO NPs improve their potential in food packaging applications. Luque et al. [70] have also synthesized ZnO NPs successfully using citrus sinensis extract. Zinc oxide nanoparticles (ZnO NPs) have emerged as prominent and versatile materials within the domain of metal oxides, garnering considerable attention across an array of scientific and industrial disciplines. Their extensive range of applications spans from enhancing industrial products [71] to revolutionizing the capabilities of sensors [10, 72], optoelectronic devices [73], biomedicine [74, 11, 9], and bioimaging [75]. On the other hand, the notable ability of PEG to deprive biological macromolecules, such as proteins and particles, from their environment, along with its exceptional activity within living organisms, is a critical factor in utilizing this polymer to create different bioconjugates [76, 77]. The features of the PEG can be attributed to the chains' significant mobility, which contributes to their capacity to adopt different conformations and bind to water. PEGylation decreases cytotoxicity and lengthens circulation time in biological contexts by improving nanoparticle dispersibility, decreasing aggregation, and minimizing protein adsorption.

In conclusion, in this work, ZnO nanoparticles were successfully synthesized using an aqueous extract of orange peel, demonstrating a sustainable approach to waste valorization in which agro-waste served as both a reducing and capping agent. The phytochemical constituents of the extract contributed beneficial properties, including enhanced biocompatibility in both in vitro and in vivo contexts, reduced nanoparticle size as confirmed by DLS and SEM analyses, and improved stability. These green-synthesized ZnO nanoparticles were further functionalized through PEGylation to obtain the final PEG-ZnO-OP formulation. In addition to their favorable biocompatibility profile, the PEG-ZnO-OP nanoparticles showed strong in vitro anticancer activity against a lung cancer cell line. Encapsulation within the polymer matrix resulted in a lower IC_{50} value compared with previously reported ZnO-based systems, indicating that effective anticancer activity could be achieved at reduced concentrations. Nonetheless, additional investigations involving other cancer cell lines and in vivo animal models are required to fully assess their therapeutic potential.

Author Contribution Statement

MK, RM, KG: Methodology, data curation, investigation, validation, writing the first draft. MK, KS, RM, KG: Resources, writing the original draft, visualization. K.G: Conceptualization, supervision, finalizing the draft.

Acknowledgements

The authors are grateful to Saveetha Institute of Medical and Technical Sciences (SIMATS), Thandalam, Chennai, India, for providing the infrastructure to conduct the experiments.

Availability of data

Data will be available on reasonable request from the corresponding author.

Ethical statement

The study was conducted in accordance with the Declaration of Helsinki, after procuring proper informed consent from the blood donor. The study was duly approved by the Institutional Ethics Committee, Saveetha Medical College and Hospital, SIMATS, Thandalam, Chennai, India. (005/07/2025/IEC/SMCH).

Experiments involving zebrafish embryos were performed after getting permission from the Institutional Animal Ethics Committee (IAEC approval No. SU/CLAR/RD/19/2025), Saveetha Medical College and Hospital, SIMATS.

Conflict of Interest

The authors declare no conflict of interest.

References

1. Deepika B, Janani G, Mercy DJ, Udayakumar S, Raghavan V, Isaac JB, et al. Assessing the anticancer potential of cerium oxide nanoparticles with doxorubicin in a polymeric nanomatrix: Histopathological and antiangiogenic insights. ChemNanoMat. 2025;11(9):e202500186. https://doi.org/10.1002/cnma.202500186.
2. Rajkumar M, Presley SD, Begum MY, Alamri A, Al Fatease A, Girigoswami K, et al. Biogenic synthesis of cuo-tio2 nanocomposites from senna auriculata (l.) roxb. Plant extract and its evaluation of antioxidant, antibacterial and anticancer activity of hepg2 cell lines. Biocatal Agric Biotechnol. 2025:103787. https://doi.org/10.1016/j.bcab.2025.103787
3. Thirumalai A, Durgadevi P, Kiran V, Girigoswami K, Prabhu AD, Girigoswami A. Lipid functionalized silver-coated carbon dot-capped manganese ferrite as drug-free core-shell nanoparticles for multimodal imaging and therapy. Admet dmpk. 2025;13(5):2905. https://doi.org/10.5599/

admet.2905.
4. Pandiarajan S, Udayakumar S, Janani G, Mercy DJ, Deepika B, Thirumalai A, et al. Anticancer effects of biomimetic green-synthesized silver nanoparticles coated lactobacilli species against various cancer cell lines. 3 Biotech. 2025;15(8):1-15. https://doi.org/10.1007/s13205-025-04393-4.
5. Irede EL, Awoyemi RF, Owolabi B, Aworinde OR, Kajola RO, Hazeez A, et al. Cutting-edge developments in zinc oxide nanoparticles: Synthesis and applications for enhanced antimicrobial and uv protection in healthcare solutions. RSC Adv. 2024;14(29):20992-1034. https://doi.org/10.1039/d4ra02452d
6. Parihar V, Raja M, Paulose R. A brief review of structural, electrical and electrochemical properties of zinc oxide nanoparticles. Rev Adv Mater Sci. 2018;53(2):119-30. https://doi.org/10.1515/rams-2018-0009
7. Kulkarni SS, Shirsat MD. Optical and structural properties of zinc oxide nanoparticles. Int J Adv Res Phys Sci. 2015;2(1):14-8.
8. Girigoswami K, Viswanathan M, Murugesan R, Girigoswami A. Studies on polymer-coated zinc oxide nanoparticles: Uv-blocking efficacy and in vivo toxicity. Mater Sci Eng C. 2015;56:501-10. https://doi.org/10.1016/j.msec.2015.07.017.
9. Girigoswami A, Deepika B, Udayakumar S, Janani G, Mercy DJ, Girigoswami K. Peony-shaped zinc oxide nanoflower synthesized via hydrothermal route exhibits promising anticancer and anti-amyloid activity. BMC Pharmacol Toxicol. 2024;25(1):101. https://doi.org/10.1186/s40360-024-00830-x.
10. Akhtar N, Metkar SK, Girigoswami A, Girigoswami K. Zno nanoflower based sensitive nano-biosensor for amyloid detection. Mater Sci Eng C. 2017;78:960-8. https://doi.org/j.msec.2017.04.118.
11. Girigoswami A, Ramalakshmi M, Akhtar N, Metkar SK, Girigoswami K. Zno nanoflower petals mediated amyloid degradation-an in vitro electrokinetic potential approach. Mater Sci Eng C. 2019;101:169-78. https://doi.org/10.1016/j.msec.2019.03.086.
12. Kalavathi R, Vijayakumar S, Dhivyadharshini S, Al-Ansari MM, Indhusha M, Soundarya S, et al. Phyco-fabricated zinc oxide nanorods from dictyota dichotoma seaweed: A promising resource for environmental and biomedical applications. Luminescence. 2025;40(7):e70272. https://doi.org/10.1002/bio.70272
13. Thenmozhi S, Dhanalakshmi J, Albeshr MF, Kumar JV, Srinivasan P, Selvi VS. Fabrication and characterization of zinc oxide nanoparticles derived from aegle marmelos fruit: Evaluation of antioxidant, antibacterial, and photocatalytic properties. Luminescence. 2025;40(6):e70224. https://doi.org/10.1002/bio.70224
14. Droepenu EK, Wee BS, Chin SF, Kok KY, Maligan MF. Zinc oxide nanoparticles synthesis methods and its effect on morphology: A review; 2022.
15. Hamada AM, Radi AA, Al-Kahtany FA, Farghaly FA. A review: Zinc oxide nanoparticles: Advantages and disadvantages. J Plant Nutr. 2024;47(4):656-79. https://doi.org/10.1080/01904167.2023.2280127
16. Naveed Ul Haq A, Nadhman A, Ullah I, Mustafa G, Yasinzai M, Khan I. Synthesis approaches of zinc oxide nanoparticles: the dilemma of ecotoxicity. Journal of Nanomaterials. 2017;2017(1):8510342.
17. Fakhari S, Jamzad M, Kabiri Fard H. Green synthesis of zinc oxide nanoparticles: A comparison. Green Chem Lett Rev. 2019;12(1):19-24. https://doi.org/10.1080/17518253.2018.1547925
18. Agarwal H, Kumar SV, Rajeshkumar S. A review on green synthesis of zinc oxide nanoparticles–an eco-friendly approach. Resource-Efficient Technologies. 2017;3(4):406-13. https://doi.org/10.1016/j.reffit.2017.03.002
19. Sampath S, Sunderam V, Madhavan Y, Hariharan N, Mohammed SSS, Muthupandian S, et al. Facile green synthesis of zinc oxide nanoparticles using artocarpus hirsutus seed extract: Spectral characterization and in vitro evaluation of their potential antibacterial-anticancer activity. Biomass Convers Bior. 2025;15(4):4969-83. https://doi.org/10.1007/s13399-023-04127-7
20. Erdoğan Ö, Paşa S, Demirbolat GM, Birtekocak F, Abbak M, Çevik Ö. Synthesis, characterization, and anticarcinogenic potent of green-synthesized zinc oxide nanoparticles via citrus aurantium aqueous peel extract. Inorg Nano-Metal Chem. 2025;55(1):67-75. https://doi.org/10.1080/24701556.2023.2240768
21. Kučuk N, Primožič M, Knez Ž, Leitgeb M. Sustainable biodegradable biopolymer-based nanoparticles for healthcare applications. Int J Mol Sci. 2023;24(4):3188. https://doi.org/10.3390/ijms24043188
22. Dumontel B, Conejo-Rodríguez V, Vallet-Regí M, Manzano M. Natural biopolymers as smart coating materials of mesoporous silica nanoparticles for drug delivery. Pharmaceutics. 2023;15(2):447. https://doi.org/10.3390/pharmaceutics15020447.
23. Gaballa SA, Naguib Y, Mady FM, Khaled KA. Polyethylene glycol: Properties, applications, and challenges. J Adv Biomedical Pharm Sci. 2024;7(1):26-36. https://doi.org/10.21608/jabps.2023.241685.1205
24. Adekoya OC, Adekoya GJ, Kupolati WK, Hamam Y, Sadiku RE. Polyethylene glycol-functionalized graphene oxide nanocomposites: Advances in biomedical applications. Nano Select. 2025:e70051. https://doi.org/10.1002/nano.70051
25. Rodriguez-Rivera GJ, Green M, Shah V, Leyendecker K, Cosgriff-Hernandez E. A user's guide to degradation testing of polyethylene glycol-based hydrogels: From in vitro to in vivo studies. J Biomed Mater Res A. 2024;112(8):1200-12. https://doi.org/10.1002/jbm.a.37609
26. Yao X, Qi C, Sun C, Huo F, Jiang X. Poly (ethylene glycol) alternatives in biomedical applications. Nano Today. 2023;48:101738. https://doi.org/10.1016/j.nantod.2022.101738
27. Caliceti P, Veronese FM. Pharmacokinetic and biodistribution properties of poly (ethylene glycol)–protein conjugates. Adv Drug Deliv Rev. 2003;55(10):1261-77. https://doi.org/10.1016/s0169-409x(03)00108-x
28. Gabizon A, Catane R, Uziely B, Kaufman B, Safra T, Cohen R, et al. Prolonged circulation time and enhanced accumulation in malignant exudates of doxorubicin encapsulated in polyethylene-glycol coated liposomes. Cancer Res.1994;54(4):987-92.
29. Hadi AJ, Nayef UM, Mutlak FAH, Jabir MS. Laser-ablated zinc oxide nanoparticles and evaluation of their antibacterial and anticancer activity against an ovarian cancer cell line: In vitro study. Plasmonics. 2023;18(6):2091-101. https://doi.org/10.1007/s11468-023-01933-7
30. Khan M, Ahmad B, Hayat K, Ullah F, Sfina N, Elhadi M, et al. Synthesis of zno and peg-zno nanoparticles (nps) with controlled size for biological evaluation. RSC Adv. 2024;14(4):2402-9. https://doi.org/10.1039/d3ra07441b
31. Zafar A, Khatoon S, Khan MJ, Abu J, Naeem A. Advancements and limitations in traditional anti-cancer therapies: A comprehensive review of surgery, chemotherapy, radiation therapy, and hormonal therapy. Discov Oncol. 2025;16(1):607. https://doi.org/10.1007/s12672-025-02198-8
32. Udayakumar S, Pandiarajan S, Jessy Mercy D, Suresh J,

Jagadeesh kumar JR, Girigoswami A, et al. Revolutionizing cancer vaccine: The power of advanced nanotechnology. Chemistry. 2025;7(3):97. https://doi.org/10.3390/chemistry7030097
33. Ratan ZA, Haidere MF, Nurunnabi M, Shahriar SM, Ahammad AS, Shim YY, et al. Green chemistry synthesis of silver nanoparticles and their potential anticancer effects. Cancers. 2020;12(4):855. https://doi.org/10.3390/cancers12040855
34. Garg P, Garg R. Qualitative and quantitative analysis of leaves and stem of tinospora cordifolia in different solvent extract. J Drug Deliv Ther. 2018;8(5-s):259-64. https://doi.org/10.22270/jddt.v8i5-s.1967.
35. Guttapalli T, RK NK, RM H, Girigoswami K. Rgo decorated with zno synthesized using clitoria ternatea flower extract-characterization, in vitro and in vivo biocompatibility, and textile dye remediation. J Compos Sci. 2025;9(9):454. https://doi.org/10.3390/jcs9090454
36. Harish S, Archana J, Navaneethan M, Silambarasan A, Nisha K, Ponnusamy S, et al. Enhanced visible light induced photocatalytic activity on the degradation of organic pollutants by sno nanoparticle decorated hierarchical zno nanostructures. RSC Advances. 2016;6(92):89721-31. https://doi.org/10.1039/C6RA19824D
37. Clogston JD, Patri AK. Zeta potential measurement. Characterization of nanoparticles intended for drug delivery. 2011:63-70.
38. Marsalek R. Particle size and zeta potential of zno. APCBEE procedia. 2014;9:13-7.
39. Bhattacharjee S. Dls and zeta potential–what they are and what they are not? J Control Release. 2016;235:337-51. https://doi.org/10.1016/j.jconrel.2016.06.017.
40. Hameed H, Waheed A, Sharif MS, Saleem M, Afreen A, Tariq M, et al. Green synthesis of zinc oxide (zno) nanoparticles from green algae and their assessment in various biological applications. Micromachines. 2023;14(5):928. https://doi.org/10.3390/mi14050928
41. Gopakumari Satheesh Chandran L, Krzemińska A, Sudararaju S, Hinder SJ, Zatylna A, Paneth P, et al. Engineering of brewery waste-derived graphene quantum dots with zno nanoparticles for treating multi-drug resistant bacterial infections. J Environ Chem Eng. 2024;12(2):112263. https://doi.org/10.1016/j.jece.2024.112263.
42. Ahmad T, Pandey V, Husain MS, Munjal S. Structural and spectroscopic analysis of pure phase hexagonal wurtzite ZnO nanoparticles synthesized by sol-gel. Materials Today: Proceedings. 2022 Jan 1;49:1694-7.
43. Deygen IM, Kudryashova EV. New versatile approach for analysis of peg content in conjugates and complexes with biomacromolecules based on ftir spectroscopy. Colloids Surf B Biointerfaces. 2016;141:36-43. https://doi.org/10.1016/j.colsurfb.2016.01.030
44. Jayarambabu N, Kumari BS, Rao KV, Prabhu Y. Germination and growth characteristics of mungbean seeds (vigna radiata l.) affected by synthesized zinc oxide nanoparticles. Int J Curr Eng Technol. 2014;4(5):3411-6.
45. Liang MK, Limo MJ, Sola-Rabada A, Roe MJ, Perry CC. New insights into the mechanism of zno formation from aqueous solutions of zinc acetate and zinc nitrate. Chem Mater. 2014;26(14):4119-29. https://doi.org/10.1021/cm501096p
46. Jiménez-Rosado M, Gomez-Zavaglia A, Guerrero A, Romero A. Green synthesis of zno nanoparticles using polyphenol extracts from pepper waste (capsicum annuum). J. Clean. Prod. 2022;350:131541. https://doi.org/10.1016/j.jclepro.2022.131541
47. Liu F, Zhang N, Wei M, Li Y, Liu X, Han Q. A systematic review of the nano-technology applied in traditional chinese medicines. Tradit Med Res. 2025;10(11):68. https://doi.org/10.53388/TMR20250124002.
48. Abdelazem RE, Hefnawy H, El-Shorbagy GA. Chemical composition and phytochemical screening of citrus sinensis (orange) peels. Zagazig J Agric Res. 2021;48(3):793-804.
49. Saleem M, Durani AI, Asari A, Ahmed M, Ahmad M, Yousaf N, et al. Investigation of antioxidant and antibacterial effects of citrus fruits peels extracts using different extracting agents: Phytochemical analysis with in silico studies. Heliyon. 2023;9(4). https://doi.org/10.1016/j.heliyon.2023.e15433
50. Akinlabu K, Owoeye T, Emetere M, Jonathan H, Owoeye D, Akinlabu P, editors. Investigation of proximate analysis and phytochemical screening of dry orange waste (citrus sinensis) extract: From agrowaste to sustainable development. IOP Conference Series: Earth and Environmental Science; 2024: IOP Publishing.
51. Oligie MHA, Eduwuirofo LO, Iyekekpolor RM, Oghomwenrhiere O, Ejimadu C, Obasuyi EI, et al. Phyto-constituents, gc-ms analysis and antifungal activity of methanol extract of sweet orange peels. NIPES J Sci Technol Res. 2023;5(2). https://doi.org/10.5281/zenodo.8010039.
52. Torkamani R, Aslibeiki B. Bulk zno, nanoparticles, nanorods and thin film: A comparative study of structural, optical and photocatalytic properties. J Cryst Growth. 2023;618:127317. https://doi.org/10.1016/j.jcrysgro.2023.127317
53. Coleman VA, Jagadish C. Basic properties and applications of zno. Zinc oxide bulk, thin films and nanostructures. Elsevier; 2006. p. 1-20.
54. Rana SB, Bhardwaj VK, Singh S, Singh A, Kaur N. Influence of surface modification by 2-aminothiophenol on optoelectronics properties of zno nanoparticles. J Exp Nanosci. 2014;9(9):877-91. https://doi.org/10.1080/17458080.2012.736640
55. MuthuKathija M, Badhusha MSM, Rama V. Green synthesis of zinc oxide nanoparticles using pisonia alba leaf extract and its antibacterial activity. Appl Surf Sci. 2023;15:100400. https://doi.org/10.1016/j.apsadv.2023.100400
56. Mohammad F, Bwatanglang IB, Al-Lohedan HA, Shaik JP, Al-Tilasi HH, Soleiman AA. Influence of surface coating towards the controlled toxicity of ZnO nanoparticles in vitro. Coatings. 2023;13(1):172.
57. Muthukumaran S, Gopalakrishnan R. Structural, ftir and photoluminescence studies of cu doped zno nanopowders by co-precipitation method. Opt Mater. 2012;34(11):1946-53. https://doi.org/10.1016/j.optmat.2012.06.004
58. Amin K, Dannenfelser RM. In vitro hemolysis: Guidance for the pharmaceutical scientist. J Pharm Sci. 2006;95(6):1173-6. https://doi.org/10.1002/jps.20627.
59. Sæbø IP, Bjørås M, Franzyk H, Helgesen E, Booth JA. Optimization of the hemolysis assay for the assessment of cytotoxicity. Int J Mol Sci. 2023;24(3):2914. https://doi.org/10.3390/ijms24032914.
60. Valdiglesias V, Alba-González A, Fernández-Bertólez N, Touzani A, Ramos-Pan L, Reis AT, et al. Effects of zinc oxide nanoparticle exposure on human glial cells and zebrafish embryos. Int J Mol Sci. 2023;24(15):12297. https://doi.org/10.3390/ijms241512297.
61. Girigoswami A, Girigoswami K. Potential applications of nanoparticles in improving the outcome of lung cancer treatment. Genes. 2023;14(7):1370. https://doi.org/10.3390/genes14071370.
62. Rani N, Rawat K, Saini M, Shrivastava A, Kandasamy G, Saini K, et al. Rod-shaped zno nanoparticles: Synthesis, comparison and in vitro evaluation of their apoptotic activity in lung cancer cells. Chem Pap. 2022;76(2):1225-38. https://

doi.org/10.1007/s11696-021-01942-y
63. Rani N, Rawat K, Shrivastava A, Yadav S, Gupta K, Saini K. In vitro study of green synthesized ZnO nanoparticles on human lung cancer cell lines. Materials Today: Proceedings. 2022 Jan 1;49:1436-42.
64. Udayakumar S, Metkar SK, Girigoswami K, Girigoswami A. Potential effect of nanoformulated iota carrageenan in Aβ1-42 disaggregation: an in vitro, in vivo and in silico study. ADMET and DMPK. 2026 Mar 6;14.
65. Janani G, Girigoswami A, Deepika B, Udayakumar S, Mercy DJ, Girigoswami K. Harnessing the anticancer potential of amphiroa anceps: Folic acid-based liposomal nanocarriers for cancer cell killing in vitro. Nanomedicine. 2026:102901. https://doi.org/10.1016/j.nano.2026.102901
66. Nurjis F, Sarwar U, Ali J, Fayyaz M, Mazhar S, Shahzad S. Ultrasound triggered in vitro release of co-loaded nanomicelles-based doxorubicin and curcumin delivery in cancer. Tradit Med Res. 2025;10(6):32. https://doi.org/10.53388/TMR20241002001.
67. Geszke-Moritz M, Moritz M. Biodegradable polymeric nanoparticle-based drug delivery systems: Comprehensive overview, perspectives and challenges. Polymers. 2024;16(17):2536. https://doi.org/10.3390/polym16172536.
68. Sakthi Devi R, Girigoswami A, Meenakshi S, Deepika B, Harini K, Gowtham P, et al. Beneficial effects of bioinspired silver nanoparticles on zebrafish embryos including a gene expression study. Admet Dmpk. 2024;12(1):177-92. https://doi.org/10.5599/admet.2102.
69. Gao Y, Xu D, Ren D, Zeng K, Wu X. Green synthesis of zinc oxide nanoparticles using citrus sinensis peel extract and application to strawberry preservation: A comparison study. Lwt. 2020;126:109297. https://doi.org/10.1016/j.lwt.2020.109297
70. Luque P, Soto-Robles C, Nava O, Gomez-Gutierrez C, Castro-Beltran A, Garrafa-Galvez H, et al. Green synthesis of zinc oxide nanoparticles using citrus sinensis extract. J Mater Sci Mater Electron. 2018;29(12):9764-70. https://doi.org/10.1007/s10854-018-9015-2
71. Yusuff AS, Popoola LT, Aderibigbe EI. Solar photocatalytic degradation of organic pollutants in textile industry wastewater by zno/pumice composite photocatalyst. J Environ Chem Eng. 2020;8(4):103907. https://doi.org/10.1016/j.jece.2020.103907
72. Beitollahi H, Tajik S, Nejad FG, Safaei M. Recent advances in zno nanostructure-based electrochemical sensors and biosensors. J Mater Chem B. 2020;8(27):5826-44. https://doi.org/10.1039/D0TB00569J
73. Liang FX, Gao Y, Xie C, Tong XW, Li ZJ, Luo LB. Recent advances in the fabrication of graphene–zno heterojunctions for optoelectronic device applications. Journal of Materials Chemistry C. 2018;6(15):3815-33. https://doi.org/10.1039/C8TC00172C
74. Weng Z, Xu Y, Gao J, Wang X. Research progress of stimuli-responsive zno-based nanomaterials in biomedical applications. Biomater Sci. 2023;11(1):76-95. https://doi.org/10.1039/D2BM01460B
75. Dey A, Ray PG, Dhara S, Neogi S. Optically engineered zno nanoparticles: Excitable at visible wavelength and lowered cytotoxicity towards bioimaging applications. Appl Surf Sci. 2022;592:153303. https://doi.org/10.1016/j.apsusc.2022.153303
76. Tiwari A, Goswami S, Joshi M, Gandhi S, Soni P, Tekade M, et al. Pegylation as a tool to alter immunological properties of nanocarriers. Pegylated nanocarriers in medicine and pharmacy. Springer; 2025. p. 171-93.
77. Mehrizi TZ, Mirzaei M, Ardestani MS. Pegylation, a successful strategy to address the storage and instability problems of blood products: Review 2011-2021. Curr Pharm Biotechnol. 2024;25(3):247-67. https://doi.org/10.2174/1389201024666230522091958.